

# DMD Analysis of Experimental PIV Data of a Swirled Jet

Lombardi, S.<sup>1</sup>, Bizon, K.<sup>1</sup>, Coghe, A.<sup>2</sup>, Cozzi, F.<sup>2</sup>, Continillo, G.<sup>1,3</sup>

<sup>1</sup>Department of Engineering, Università del Sannio  
Benevento, Italy

<sup>2</sup>Department of Energy, Politecnico di Milano, Italy

<sup>3</sup>Istituto Motori CNR, Naples, Italy

## 1 Abstract

This paper concerns the study of high Reynolds and high swirl number flow through the use of PIV measurements and Dynamic Mode Decomposition (DMD) analysis. Principles governing DMD are briefly recalled, then the use of DMD is demonstrated by analysing the acquired PIV data in order to study the dominant dynamics of the system and extracting relevant morphology via DMD modes, focusing the attention on phenomenon known as Precessing Vortex Core (PVC).

## 2 Introduction

Swirl flows are widely used in several technical applications such as cyclone separators, gas turbine combustors, hybrid rockets etc. etc. [1]. For example, in combustion processes the high turbulence levels and the recirculating flow observed at high swirl levels greatly improve reactants mixing and flame stability, while allowing the reduction of pollutant emissions. Improvement in these technical applications requires a deeper understanding of the dynamics of swirling flows, whose features are still debated by the scientific community. One peculiar phenomenon of swirl flows is the so-called Precessing Vortex Core (PVC). The PVC occurs in high Reynolds and swirl number flows and is characterized by the regular precession of the large-scale vortical structure typical of swirling jets around the geometrical axis of symmetry [1]. An analysis of the 3D and unsteady flow structure of the PVC can be found in the experimental works of Cala et al. [2-3] and Shtork [4], while a review of PVC instability in swirl combustion systems can be found in [5].

A common technique to identify the coherent features in a field is the Proper Orthogonal Decomposition (POD) [6]. Bizon et al. [7-8] proposed a method based on POD and gaussianity indexes, in order to separate coherent and incoherent components regarding combustion processes within internal combustion engines. Another decomposition technique recently applied to the analysis of combustion phenomena is ICA [9-10].

This work describes the application of Dynamic Mode Decomposition (DMD) to PIV measurements of a swirled jet in order to identify and characterize the dominant dynamic components of the system.

### 3 Experimental

The investigated flow is a turbulent free swirling jet of air at ambient pressure and temperature. The swirl generator was of axial plus-tangential entry type characterized by four axial and four tangential air inlets. A converging nozzle of exit radius  $R=12$  mm was located vertically on top of the swirl generator. A circular pipe having an inner radius  $R_{inj}=6$  mm was located coaxially to the swirl generator and used for flow seeding. Its exit section was set at about  $26 R_{inj}$  below the nozzle exit. A schematic view of the nozzle is shown in Fig. 1, while a detailed drawing of the swirl generator is reported in [11]. The total air flow rate and the swirl strength were regulated by controlling the flow rates in the seeding system, the axial and the tangential entries by using thermal mass flowmeters whose error was estimated around  $\pm 1\%$  of the full scale.

The seeding system generates oil droplets with an estimated diameter of about  $1-2 \mu\text{m}$ . The maximum measurable frequency of the flow fluctuations, limited by the inertia of the tracer particles, was estimated to be around  $12.7$  kHz, while the Stokes number estimation allowed to assume that the centrifugal effect on tracer particles was negligibly small [11].

PIV measurements were performed using a high speed double pulsed Nd:YLF laser operating at  $527$  nm. Double images were acquired with a CMOS (Dantec NanoSense MKIII) cross-correlation PIV camera with a full resolution of  $1280 \times 1024$  pixels. The spatial resolution in the direction normal to the measurement plane was estimated from the average thickness of the laser sheet, which was about  $1$  mm. The laser sheet was located normally to the nozzle axis and at about  $1$  mm above the nozzle exit, (see Fig. 1). At the investigated swirl and Reynolds numbers the jet exhibits a Precessing Vortex Core (PVC) with a frequency of about  $486$  Hz [12], thus, to fulfill the Nyquist-Shannon sampling theorem, PIV images were acquired at about three times the PVC frequency, i.e.  $1500$  double images/s, while the interframe time was set to  $10 \mu\text{s}$ . The camera operates at the (reduced) resolution of  $640 \times 640$  pixels corresponding to a field of view of about  $33 \times 33 \text{ mm}^2$  and a magnification of  $0.305$ .

PIV images were processed by means of the Dantec software. The size of the interrogation area was set to  $32 \times 32$  pixels corresponding to a spatial resolution of about  $1.2$  mm. An overlap of  $50\%$  was used. The velocity maps were vector-validated basing on the cross-correlation peak height ratio and on the velocity magnitude. The statistical error relative to the mean value of the velocity is estimated to be less than  $3\%$  for the  $1000$  couples of images acquired.

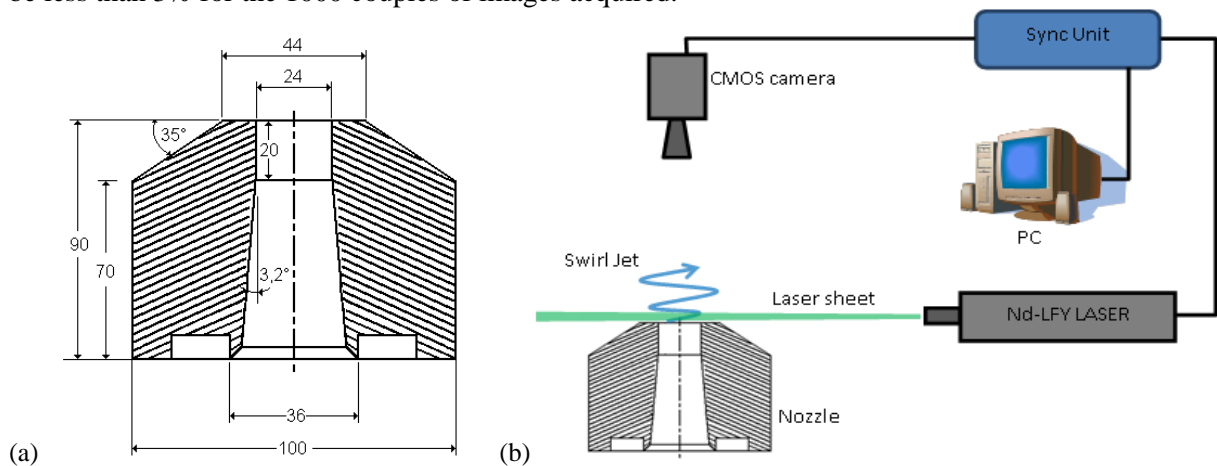


Fig. 1: Schematic of the nozzle, all dimension in mm (a). Sketch of the experimental set-up (b).

### 4 Dynamic Mode Decomposition

Dynamic Mode Decomposition (DMD) is a recent analysis technique proposed by Schmid [13] to extract useful information from experimental and simulation data in terms of frequency and growth rate of coherent spatial features. Particularly, DMD is based on the Koopman analysis [14] of dynamical systems. It permits to extract spatial modes (spatial features) from a given data set

(snapshots) and to associate to each mode a unique frequency and a growth rate (temporal feature). In last years, many researchers have used DMD to extract and describe the underlying phenomena from set of data obtained by particle image velocimetry (PIV) experiments and large eddy simulations (LES). Schmid et al. [15] applied DMD to Schlieren snapshots of a helium jet and to time-resolved PIV-measurements of an unforced and harmonically forced jet, to analyse the physical mechanism of the fluid flow. Seena and Snug [16] used DMD to carry out the global stability analysis on cavity flow at high Reynolds numbers, in order to extract the features of the flow field that may be related to flow instability. In this section, we follow the same mathematical description made by Schmid [13] on the DMD. Given a sequence of snapshots obtained by experiments or simulations,  $\mathbf{v}_i$ , it is possible to organize the data into the following matrix:

$$\mathbf{V}_1^N = \{\mathbf{v}_1, \mathbf{v}_2, \dots, \mathbf{v}_N\} \quad (1)$$

The subscript, 1 in this case, denotes the first snapshot of the sequence, while the superscript,  $N$  in this case, denotes the last snapshot of the sequence. Besides, we assume an ordered sequence of snapshots uniformly sampled with a constant period. The main idea of DMD is to assume the existence of a constant linear mapping  $\mathbf{A}$  relating each  $\mathbf{v}_i$  to the subsequent snapshot  $\mathbf{v}_{i+1}$ , that is  $\mathbf{v}_{i+1} = \mathbf{A}\mathbf{v}_i$ , such that it is possible to consider  $\mathbf{V}_1^N$  as a Krylov sequence:

$$\mathbf{V}_1^N = \{\mathbf{v}_1, \mathbf{A}\mathbf{v}_1, \mathbf{A}^2\mathbf{v}_1, \dots, \mathbf{A}^{N-1}\mathbf{v}_1\} \quad (2)$$

The objective of DMD is the extraction of the dynamic characteristics of a given dynamical process described by  $\mathbf{A}$ , which is based on the snapshot sequence  $\mathbf{V}_1^N$ . It is reasonable to assume that it exists a critical number of snapshots, say  $N$ , beyond which the vector components of  $\mathbf{V}_1^N$  become linearly dependent. Then, it is acceptable to express the snapshot  $\mathbf{v}_N$  as a linear combination of the  $N-1$  previous linearly independent snapshots, that is  $\mathbf{v}_N = \mathbf{V}_1^{N-1}\mathbf{a} + \mathbf{r}$ , where  $\mathbf{a} = \{a_1, a_2, \dots, a_N\}$  and  $\mathbf{r}$  is the vector residual. By following Ruhe [17], we can write:  $\mathbf{V}_2^N = \mathbf{A}\mathbf{V}_1^{N-1} = \mathbf{V}_1^{N-1}\mathbf{S} + \mathbf{r}$  where, as mentioned in Schmid [13],  $\mathbf{S}$  is the companion matrix of the polynomial  $\mathbf{V}_1^{N-1}\mathbf{a}$ . Therefore, it is clear that, as the residual  $\mathbf{r}$  becomes smaller and smaller, the eigenvalues of  $\mathbf{S}$  approximate better and better the eigenvalues of  $\mathbf{A}$ . Thus, DMD can be considered as an optimization problem with the following objective:

$$\mathbf{S} = \arg \min_{\mathbf{M}} \|\mathbf{V}_2^N - \mathbf{V}_1^{N-1}\mathbf{M}\| \quad \text{with } \mathbf{M} \in \mathbb{R}^{(N-1) \times (N-1)} \quad (3)$$

The optimal solution of Eq. (4) can be found following Schmid [13]. Here  $\mathbf{S}\mathbf{y}_i = \lambda_i\mathbf{y}_i$  with  $\mathbf{y}_i$  and  $\lambda_i$  being, respectively, the  $i$ -th eigenvector and eigenvalue (they are typically complex and conjugate) of  $\mathbf{S}$ . Each  $i$ -th dynamic mode ( $DM_i$ ),  $\phi_i$ , is then obtained by projection of  $\mathbf{V}_1^{N-1}$  onto the eigenvector  $\mathbf{y}_i$ , namely:

$$\phi_i = \mathbf{V}_1^{N-1}\mathbf{y}_i \quad i = 1, 2, \dots, N \quad (4)$$

The information about the frequency,  $f_i$ , and growth rate,  $\sigma_i$ , of each dynamic mode are provided by the eigenvalues  $\lambda_i$  through the following relationships:

$$\sigma_i = \log(|\lambda_i|) / \Delta t \quad ; \quad f_i = \arg(\lambda_i) / 2\pi\Delta t \quad (5)$$

whereas the amplitude of the  $i$ -th dynamic mode is given by its  $L_2$ -norm,  $\|\phi_i\|_{L_2}$ . Hence, it is clear that

DMD provides information about the dynamics of the system in terms of spatial features (dynamic modes) corresponding to a particular frequency and growth rate. Moreover, in the case of unstable phenomena, this decomposition can provide information about the stability of the system, and identify the spatial features that may be due to instability, as shown in [18]. In fact, the dynamic modes connected to instabilities are characterized by growth rate values higher than unity.

## 5 Results and discussion

Figure 2 shows representative snapshots of the PIV velocity field, with clear evidence of the PVC. DMD applied to the PIV data elucidates the dynamics connected with vortex motion and other transient phenomena. Figure 3 reports, in the complex plane, the spectrum of the companion matrix  $\mathbf{S}$  (Eq. 3), where it is seen that all eigenvalues tend to localize close to the unit circle. Figure 3 (left) shows the eigenvalues of  $\mathbf{S}$ . As expected, there are many complex and conjugate eigenvalues, due to the oscillating dynamics. The radius of each data marker corresponds to the square amplitude of the mode, i.e. the amount of kinetic energy of the flow captured by the dynamic mode. Most of the kinetic energy of the flow is captured by mode DM0, namely the mean component, and by one pair of complex-conjugate modes, DM2 and DM2\*, associated with the main precessing vortex.

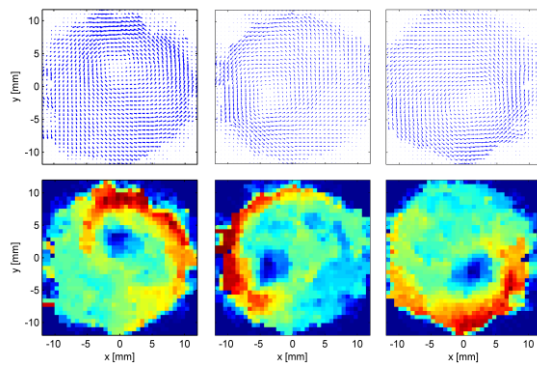


Figure 2. Representative snapshots of the arrow field velocity maps (top) and their moduli shown as scalar fields (bottom).

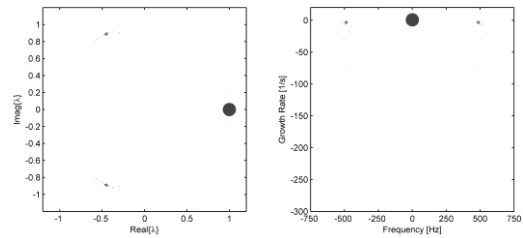


Figure 3. DMD analysis using the last 300 snapshots. (Left) Scatter plots of the eigenvalues of  $\mathbf{S}$ . (Right) Scatter plots of the normalized growth rates versus normalized frequencies for all dynamic modes. In both scatter plots, size of the circle denote the amount of energy captured by dynamic mode.

In order to analyse transient phenomena that may be captured by the PIV dataset, DMD was carried out on different numbers of snapshots, namely for different observation times. Particularly, two ensembles of snapshot were studied by DMD. The first set is made up of 1000 snapshots (i.e. the entire sequence of snapshots), and the second one is made up of the last 300 snapshots of the entire sequence. Figure 4 shows the amplitude spectra of the dynamic modes relating to the two sequences (1000 and 300 snapshots). It is possible to notice that the dynamic mode DM1 occurs, with significant amplitude, only for the case of 1000 snapshots, namely when the time interval includes the early transient. Indeed, DM1 is not observed for the sequence made of the last 300 snapshots. Figure 5 shows the spatial features associated with dynamic modes DM0 and DM1. Since DM0 has both zero growth rate and zero frequency, DM0 is associated with the mean component. Mode DM1 has significant values of amplitude and growth rate, therefore it is associated with a transient phenomenon. Precisely, the normalized growth rate of DM1 is about  $-7.95 \text{ s}^{-1}$ , which corresponds to a half-time of about 175.3 ms, and to about 20% of the amplitude of the mean component. For these reasons, DM1 can be considered as a marker of the transient condition of the system.

In Fig. 5 we look at the morphology of the first four modes. We see that DM0 is axisymmetric as it should be, dealing with a conical swirled jet. DM1 is roughly axisymmetric as well, and peaks near the edge of the jet. This indicates that the main transient component of the flow is related to viscous phenomena that decay in amplitude whilst maintaining axisymmetric structure. The spiral patterns of the paired modes associated with the precessing vortex are also reported.

In Fig. 3 it is possible to see a cloud of minor modes in a neighbourhood of the normalized frequencies of the pair of dominant conjugate modes associated with the precessing vortex, however only one dominant pair of dynamic modes (DM2, DM2\*) are related to the precessing vortex, with frequency of

486 Hz for both samples. DM1, detected as the second largest in the set of first 1000 snapshots, disappears in the set of last 300 snapshots. The mean component (DM0) and the precessing vortex (DM2 and DM2\*) are identified by the three largest circles in Fig. 3 and the three highest spikes in Fig. 4, and are present in both spectra, the one obtained by 1000 snapshots and the one obtained by using the last 300 only. Finally, since all growth rates are negative, or, equivalently, the eigenvalues of  $\mathbf{S}$  are less than unity in absolute value, the dynamics of the system can be considered stable.

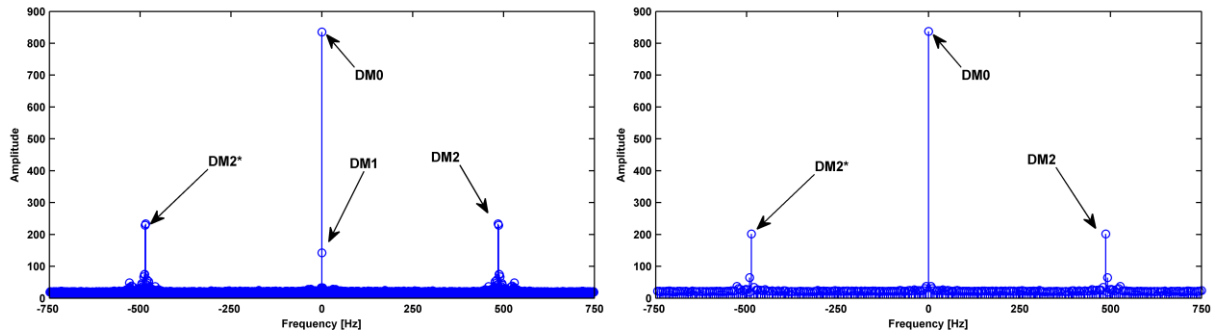


Figure 4. Spectrum of the DMD modes for 1000 snapshots (right) and last 300 snapshots (left).

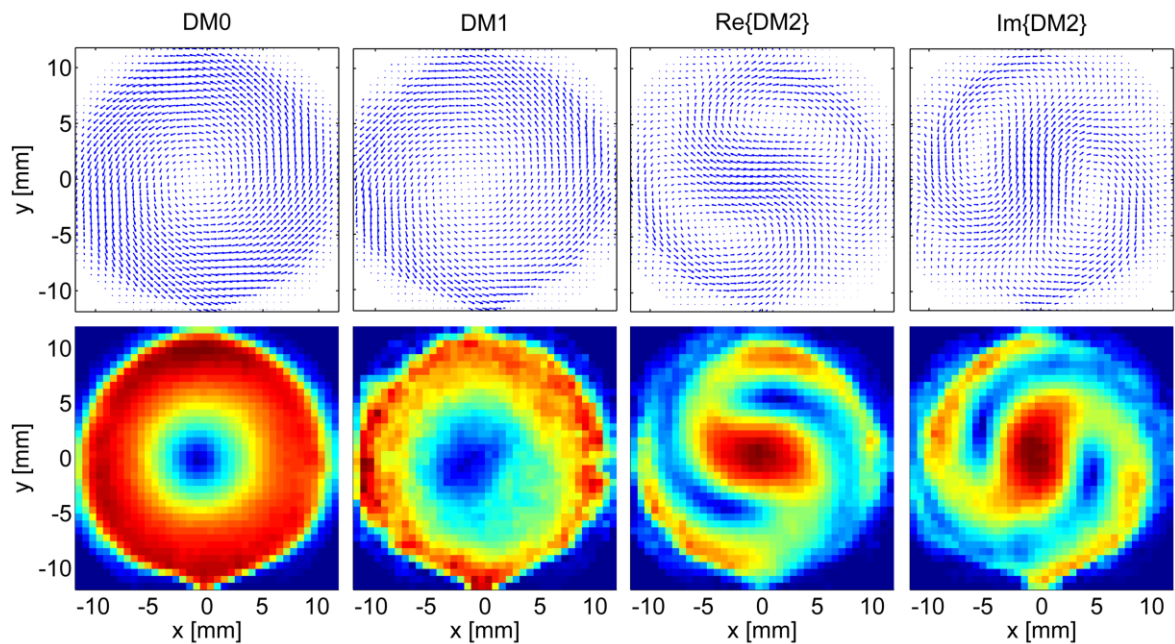


Figure 5 - Velocity maps (top row) and dynamic modes in terms of velocity moduli (bottom row).

## 6 Conclusions

Dynamic Mode Decomposition proved to be instrumental in characterizing the dynamics of the precessing vortex core in a swirled jet flow, by using the set of PIV snapshots collected. DMD identified the features of the precessing vortex in terms of frequency, growth rate and morphology (spatial pattern described by the dynamic modes), and even allowed to identify the feature associated with a transient phenomenon. On account of the determined eigenvalues, the system can be considered dynamically stable.

## References

- [1] Gupta AK, Lilley DG, Syred N., Swirl Flows, Abacus Press, Tunbridge Wells, 1984.
- [2] Cala C.E., Fernandes E.C., Heitor M.V., Shtork S.I., LDA analysis of PVC-central recirculation zone interaction in a model vortex burner. 12th Int. Symp. On Applications of Laser Techniques, Lisbon, July 2004.
- [3] Cala C.E., Fernandes E.C., Heitor M.V., Shtork S.I. (2006). Coherent structures in unsteady swirling jet flow. *Experiments in Fluids* 40, 267–276.
- [4] Shtork S. I., Cala C. E. and Fernandes E. C. (2007). Experimental characterization of rotating flow field in a model vortex burner. *Exp Therm Fluid Sci* 31(7), 779-788.
- [5] Syred N. (2006). A review of oscillation mechanisms and the role of the precessing vortex core (PVC) in swirl combustion systems. *Progr Energy and Comb Science* 32, 93–161.
- [6] Holmes P., Lumley J.L. and Berkooz G. (1998) *Turbulence, Coherent Structures, Dynamical Systems and Symmetry*, Cambridge University Press, Cambridge, UK, p. 186.
- [7] Bizon K., Continillo G., Leistner K.C., Mancaruso E. and Vaglieco B.M. (2009). POD-based analysis of cycle-to-cycle variations in an optically accessible diesel engine. *Proc. of the Combustion Institute*. 32, 2809-2816.
- [8] Bizon K., Continillo G., Mancaruso E., Merola S.S. and Vaglieco B.M. (2010). POD-based analysis of combustion images in optically accessible engines. *Combustion and Flame* 157, 632-640.
- [9] Bizon K., Lombardi S., Continillo G., Mancaruso E., Vaglieco B.M. (2013). Analysis of Diesel engine combustion using imaging and independent component analysis. *Proc. of the Combustion Institute* 34 (2), 2921-2931.
- [10] Bizon K., Continillo G., Lombardi S., Mancaruso E., Sementa P. and Vaglieco B.M. (2014). Independent component analysis Applied to combustion images in transparent engines. *Ingineri automobilului* 8(30).
- [11] Martinelli F., Olivani A. and Coghe A. (2007). Experimental Analysis of the Precessing Vortex Core in a Free Swirling Jet. *Experiments in Fluids* 42, 827-839.
- [12] Martinelli F., Cozzi F. and Coghe A. (2012). Phase-locked analysis of velocity fluctuations in a turbulent free swirling jet after vortex break down, *Exp Fluids*, 53, 437-449.
- [13] Schmid P.J. (2010). Dynamic mode decomposition of numerical and experimental data. *J. Fluid Mech.* (2010) 656, 5-28.
- [14] Rowley C.W., Mezić I., Baghieri, S., Schatter, P., Hennigson D.S. (2009). Spectral analysis of nonlinear flows. *J. Fluid Mech.* 641, 115-127
- [15] Schmid P.J., Li, L., Juniper M.P., Pust O. (2010). Applications of the dynamic mode decomposition. *Theor. Comput. Fluid Dyn.* 25, 249-259.
- [16] Seena A., Sung H.J. (2011). Dynamic mode decomposition of turbulent cavity flows for self-sustained oscillations. *International Journal of Heat and Fluid Flow* 32, 1098-1110.
- [17] Ruhe A. (1984). Rational Krylov sequence methods for eigenvalue computation. *Linear Algebra Appl.* 58, 279-316.
- [18] Zhang Q., Liu Y., Wang S. (2014). The identification of coherent structures using proper orthogonal decomposition and dynamic mode decomposition. *Journal of Fluids and Structures* 49, 53-72.